A Numerical Solution of Transport of Mono- and Tri-valent Cations during Steady Water Flow in a Binary Exchange System

Hee-Myong Ro* and Sun-Ho Yoo[1]

Department of Horticultural Environment, National Horticultural Research Institute, Suwon 440-310
[1]Department of Agricultural Chemistry, Seoul National University, Suwon 441-744, Korea

Received February 25, 2000

A one-dimensional transport of displacing monovalent ion, A^+, and a trivalent ion being displaced, B^{3+}, in a porous exchange system such as soil was approximated using the Crank-Nicolson implicit finite difference technique and the Thomas algorithm in tandem. The variations in the concentration profiles were investigated by varying the ion-exchange equilibrium constant (k) of ion-exchange reactions, the influent concentrations, and the cation exchange capacity (CEC) of the exchanger, under constant flux condition of pore water and dispersion coefficient. A higher value of k resulted in a greater removal of the native ion, behind the sharper advancing front of displacing ion, while the magnitude of the penetration distance of A^+ was not great. As the CEC increased, the equivalent fraction of B^{3+} initially in the soil was greater, thus indicating that a higher CEC adsorbed trivalent cations preferentially over monovalent ions. Mass balance error from simulation results was less than 1%, indicating this model accounted for instantaneous charge balance fairly well.

Key words : *cation exchange, cubic equation, retardation, transport, trivalent.*

During advection and diffusion of fertilizers into soil, soil cations at exchange sites of soil particles are displaced and subject to leaching. Cation leaching through soil is undoubtedly complicated due not only to its physical attributes associated with soil matrix, but also to a number of chemical processes that, in turn, influence ion activities in the soil solution. In particular, cation leaching process in either acidic or volcanic ash-derived soil becomes further complicated, since trivalent cation species such as Al^{3+} and Fe^{3+} in solution phase undergo protonation. Hence, it gives a series of hydrolytic ion complexes of lesser valences and the proton, in turn, modifies the mole fraction of each hydrolytic ion species in solution phase.[1] During transport of cations through soil, multiple species of cations compete for the exchange sites of soil and those in mobile solution phase move through the soil to a direction where an individual concentration gradient has been established.[2]

The transport of cation species through soils has typically been examined and modeled as an instantaneous process. A multi-ionic transport model with assumptions of instantaneous exchange, constant exchange selectivity coefficients for each binary pair of competing ion species, constant cation exchange capacity, variable total solution concentration, and steady water flow was presented by Rubin and James.[3]

*Corresponding author
Phone: 82-331-240-3716; Fax: 82-331-240-3556
E-mail: hmro@unitel.co.kr

Abbreviations: CEC, cation exchange capacity; k, ion-exchange equilibrium constant.

Cation exchange reaction is governed by the CEC of the exchanger and the equilibrium constant or the selectivity coefficient which is commonly known to vary with equivalent fraction of cation species and their total concentration in the solution phase.[4] Some equilibrium constants or selectivity coefficients for exchange involving each binary pair of monovalent and trivalent cation species are available in the published literature.[5,6] Bond and Philips[7] asserted that spatial and temporal changes in total solution concentration during transient, unsaturated water flow in soils, however, may have minimal impact on the transport of binary heterovalent cation system. In describing multi-ionic transport in soils, at least each binary cation exchange between competing ion species should be coupled into individual advective-disperse process, since the transport of multiple cation species in soil-water system could be regarded as a set of binary combinations of cations.[2] Bond and Verburg attempted to predict ternary and higher cation exchange from binary isotherms because it is impossible to measure isotherms for all possible combinations when there are three or more competing ions.[8]

Using binary exchange relations between two competing ion species, mathematical formulations between each binary combination of cation exchange reactions have been suggested in many models. To date, however, relatively few attempts on mathematical formulation for the ion exchange reaction of trivalent cation with other cation species and their transport have been reported in the published literature.[7,9] Reuss and Johnson[10] presented a numerical model for the displacement of Al-saturated soil with solution containing divalent Ca^{2+}. However, a mathematical formulation of

binary transport of monovalent-trivalent cations with cation exchange is scarcely found in the literature.

In this investigation, protonation due to hydrolysis of trivalent cation species was not taken into account. This exclusion of hydrolysis of trivalent cation species is evidenced by the fact that an exotic trivalent cation species, La, occurs in rare-earth minerals such as monazite and bastnasite up to 22 and 32%, respectively.[11] The objectives of this study was to present a mathematical model for describing ion exchange between monovalent and trivalent cation species and their transport in steady flow conditions.

Mathematical Model

A one-dimensional form of the transport equation similar to that previously presented by Rubin and James[3] was used in this model for describing advective-diffusive transport of two competing cation species during steady water flow in porous media. The two simultaneous nonlinear partial differential equations are required to describe cation exchange and transport of displacing monovalent cation, A^+, and trivalent cations being displaced, B^{3+};

$$\frac{\partial A}{\partial t} = D\frac{\partial^2 A}{\partial z^2} - v\frac{\partial B}{\partial z} - \frac{\partial S_A}{\partial t} \tag{1}$$

$$\frac{\partial B}{\partial t} = D\frac{\partial^2 B}{\partial z^2} - v\frac{\partial B}{\partial z} - \frac{\partial S_B}{\partial t} \tag{2}$$

where D is the dispersion coefficient for both A and B species ($m^2\ s^{-1}$), v is the average pore water velocity ($m\ s^{-1}$), and t and z are time (s) and distance (m) in Cartesian coordinates, respectively. In Eqs. (1) and (2), S_A and S_B stand for the concentrations of cations in the exchange phases ($mol\ m^{-3}$), and A and B for those in solution phases ($mol\ m^{-3}$) of A and B, respectively.

In order to solve Eqs. (1) and (2), it is necessary to eliminate S_A and S_B from the equations. To do so, an equilibrium constant of binary cation exchange reaction (Eq. (3)) was introduced.

$$3A^+ + B\text{-}soil \leftrightarrow B^{3+} + A_3\text{-}Soil \tag{3}$$

In this investigation, the equilibrium constant for cation exchange is shown in Eq. (4).

$$k = \frac{(\gamma_B)^1}{(\gamma_A)^3}\left(\frac{S_A}{A}\right)^3\left(\frac{S_B}{B}\right)^{-1} \tag{4}$$

where γ_A and γ_B are the activity coefficients for ion A and B in the solution phase.

The substitution of the relation expressing the ionic composition of the adsorbed cations to satisfy the electroneutrality of the exchanger

$$S_A + 3S_B = R \tag{5}$$

into Eq. (4) results in

$$S_A^3 + \frac{KA^3}{3B}S_A - \frac{KRA^3}{3B} = 0 \tag{6}$$

where R is the cation exchange capacity of soil.

Following the mathematical procedure described by Beyer,[12] a real root of cubic Eq. (6) could be analytically obtained as

$$S_A = \sqrt[3]{y\left(R + \sqrt{R^2 + \frac{8}{27}y}\right)} - \sqrt[3]{y\left(\sqrt{R^2 + \frac{8}{27}y} - R\right)} \tag{7}$$

where

$$y = \frac{KA^3}{6B} \tag{8}$$

The last term of right-hand side of Eq. (1) can be obtained by taking the partial derivative of S_A (Eq. (7)) with respect to time, since the concentration of both A and B in solution phase is a function of time and distance. By chain rule, differentiation of Eq. (7) with respect to time can be expressed as

$$\frac{\partial S_A}{\partial t} = \left(\frac{\partial S_A}{\partial y}\right)\left(\frac{\partial y}{\partial t}\right) = \left(\frac{\partial S_A}{\partial y}\right)\left\{\left(\frac{KA^2}{2B}\right)\left(\frac{\partial A}{\partial t}\right) - \left(\frac{KA^3}{6B^2}\right)\left(\frac{\partial B}{\partial t}\right)\right\} \tag{9}$$

where

$$\frac{\partial S_A}{\partial y} = \frac{1}{3\sqrt[3]{\left\{y\left(R + \sqrt{R^2 + \frac{8}{27}y}\right)\right\}^2}}\left(R + \sqrt{R^2 + \frac{8}{27}y} + \frac{4y}{27\sqrt{R^2 + \frac{8}{27}y}}\right) - \frac{1}{3\sqrt[3]{\left\{y\left(\sqrt{R^2 + \frac{8}{27}y} - R\right)\right\}^2}}\left(\sqrt{R^2 + \frac{8}{27}y} - R + \frac{4y}{27\sqrt{R^2 + \frac{8}{27}y}}\right) \tag{10}$$

Substitution of Eq. (9) into Eq. (1) results in

$$\frac{\partial A}{\partial t} = \left(\frac{D}{1 + u_1}\right)\frac{\partial^2 A}{\partial z^2} - \left(\frac{v}{1 + u_1}\right)\frac{\partial A}{\partial z} + f_1\frac{\partial B}{\partial t} \tag{11}$$

where

$$u_1 = \left(\frac{\partial S_A}{\partial y}\right)\frac{KA^2}{2B};\ f_1 = \frac{\left(\frac{\partial S_A}{\partial y}\right)\frac{KA^3}{6B^2}}{1 + \left(\frac{\partial S_A}{\partial y}\right)\frac{KA^2}{2B}} \tag{12}$$

For the trivalent cation, a similar equation to Eq. (11) can be obtained by differentiating Eq. (5) with respect to time and substituting it into Eq. (2):

$$\frac{\partial B}{\partial t} = \left(\frac{D}{1+u_3}\right)\frac{\partial^2 B}{\partial z^2} - \left(\frac{v}{1+u_3}\right)\frac{\partial B}{\partial z} + f_3\frac{\partial A}{\partial t} \quad (13)$$

where

$$u_3 = \left(\frac{\partial S_A}{\partial y}\right)\frac{KA^3}{18B^2};\ f_3 = \frac{\left(\frac{\partial S_A}{\partial y}\right)\frac{KA^2}{2B^2}}{3\left\{1+\left(\frac{\partial S_A}{\partial y}\right)\frac{KA^3}{18B^2}\right\}} \quad (14)$$

Initial and boundary conditions for Eqs. (1) and (2), similar to those of the model presented by Cho,[13] were employed in this simulation.

$$A(z,t) = A_i,\ B(z,t) = B_i \ \ for\ 0<z<1,\ t = o \quad (15A)$$

$$S_A \cong 0,\ S_B \cong R \ \ for\ 0<z<1,\ t = o \quad (15B)$$

$$vA_o - vA + D\frac{\partial A}{\partial z} = vB_o - vB_o + D\frac{\partial B}{\partial z} = 0 \ \ for\ z=0,\ t\geq 0 \quad (15C)$$

$$\frac{dA}{dz} = \frac{dB}{dz} = 0 \ \ for\ z=1,\ t\geq 0 \quad (15D)$$

These conditions correspond to the situation in which a solution of A with concentration A_o is fed into a soil column that is initially saturated with B. Initial concentrations for each cation species in the soil must be specified for the solution and exchange phases. As boundary conditions at both ends, Neumann condition, a second-kind boundary condition, was chosen to specify the flow through the boundaries. Constant flux boundary at left and no flux boundary at right for both A and B were chosen for this investigation. Solutions of Eqs. (11) and (13) subject to Eq. (15) were numerically approximated using the Crank-Nicolson implicit finite difference technique and the Thomas algorithm in tandem. Such numerical process is unconditionally stable as long as Δt is held constant in each step.[14]

Implicit finite difference equations using the Crank-Nicolson approximation, after rearranging are

$$P_1 A_{i+1}^{j+1} - \{P_1 + P_2 + (1+u_1)\}A_i^{j+1} + P_2 A_{i-1}^{j+1} = -P_1 A_{i+1}^{j} + \{P_1 + P_2 - (1+u_1)\}A_i^{j} - P_2 A_{i-1}^{j} - 3u_3\Delta t(B_i^{j+1} - B_i^{j}) \quad (16A)$$

and

$$P_1 B_{i+1}^{j+1} - \{P_1 + P_2 + (1+u_3)\}B_i^{j+1} + P_2 B_{i-1}^{j+1} = -P_1 B_{i+1}^{j} + \{P_1 + P_2 - (1+u_3)\}B_i^{j} - P_2 B_{i-1}^{j} - \frac{1}{3}u_1\Delta t(A_i^{j+1} - A_i^{j}) \quad (16B)$$

where

$$P_1 = \frac{D\Delta t}{2(\Delta z)^2} - \frac{v\Delta t}{4\Delta z},\ P_2 = \frac{D\Delta t}{2(\Delta z)^2} + \frac{v\Delta t}{4\Delta z} \quad (17)$$

In Eqs. (16A) and (16B), i = 1, 2, ..., n is a grid point in the z-direction and j = 1, 2, ..., m is a grid point in the t-direction, and Δz and Δt are incremental distance and time, respectively. Initial conditions determine the values of A and B at j = 1, while two boundary conditions eliminate the values of A_{i-1} at i = 1 and A_{i+1} at i = n. An implicit approximation of Eqs. (11) and (13) by Crank-Nicolson method results in a set of simultaneous linear algebraic equations of (16A) and (16B) for a fixed time value of j. Since the coefficient matrix of Eq. (16) is tridiagonal, Gaussian elimination is particularly simple for such linear systems. To solve such a tridiagonal system in an efficient manner, a variation on Gaussian elimination, frequently referred to as the Thomas algorithm, was also applied in this model.

Results and Discussion

Variations in cation concentration profiles. With the arbitrary input values of parameters (Table 1), spatial and temporal distributions of concentration of displacing ion, A^+, and the displaced ion, B^{3+}, in solution corresponding to the several chosen times were numerically simulated in Fig. 1. In the model, the cation exchange capacity, R, expressed on soil mass basis was converted to that on solution basis expressed in the same units as A and B (mol m^{-3}).[13] One

Table 1. Physical and ion-exchange parameters as standard input variables for dispersion model.

Parameter	Values
Exchanger bulk density, ρ_b	1.30 Mg m^{-3}
Initial water content, θ_m	0.20 kg kg^{-1}
Dispersion coefficient, D	1×10^{-9} m^2 s^{-1}
Pore water velocity, v	1×10^{-6} m s^{-1}
Binary cation exchange capacity, R	1 cmol kg^{-1}
Equilibrium constant, k	1
Incremental time, Δt	1 s
Incremental distance, Δz	0.002 m

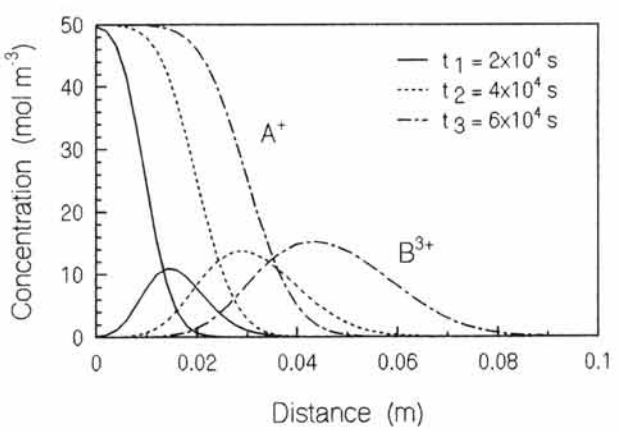

Fig. 1. Distributions of A^+ and B^{3+} in solution at different times with standard input parameters of dispersion model.

cmol kg^{-1} of the CEC of the soil whose gravimetric moisture content is 0.2 kg kg^{-1} and bulk density 1.3 Mg m^{-3} corresponds to 50 mol m^{-3}, since gravimetric moisture content multiplied by bulk density yields volumetric moisture content.

As the invading ion, A^+, advanced into the soil, the ion, B^{3+}, was displaced from the soil exchanger and its concentration in the soil solution increased to the maximum concentration just ahead of the advancing front of incoming ion, A^+. However, the position of the maximum of the displaced ion, B^{3+}, was behind the position of the advancement of pore water. A buildup of native exchangeable cations in the solution phase and the retardation in the movement of invading cation was observed in Fig. 1. The average pore water velocity was chosen to be 1×10^{-6} m s^{-1} (Table 1) and the average velocity of advancing front of A^+ was nearly 5×10^{-7} m s^{-1}, which is approximately one half that of water.

Unlike the invading ion, A^+, the concentration of B^{3+} in solution decreased along both shoulders of the curve from its peak concentration. However, the overall picture of spatial distribution of two species was not changed once the transport process was initiated, but the maximum concentration of B^{3+} in solution and the distance its position traveled became larger as time advanced. The average velocity of the left shoulder of the curve was nearly 5×10^{-7} m s^{-1}, while the right shoulder moved with the same velocity of pore water. This discrepancy in the average velocities of both shoulders results in asymmetrical distribution, making it appear that the position of the maximum would travel with the average velocity of 7.5×10^{-7} m s^{-1}.

The distance between the adjacent curves of B^{3+} at different times on the right side of the maximum are twice as large as those on the left side of the maximum. On the other hand, the distance of separation of the adjacent curves of A^+ and B^{3+} are equal on the left side of the maximum. Thus, the average velocity of B^{3+} appearing on the right side of the maximum is approximately double the velocity of A^+, thus indicating B^{3+}, once displaced from the exchange site of the soil, does not undergo exchange reaction beyond the displacement zone and satisfies the initial saturation of exchange complex with B^{3+}.

Influence of exchange equilibrium constant. Under the conditions where cation exchange capacity, dispersion coefficient, and the velocity of pore water movement are kept constant, the magnitude of transport of both A^+ and B^{3+} was greatly modified by the affinity of cation species towards the exchanger (Fig. 2). Calculation using value of $k = 0.1$ showed that the distribution patterns of both A^+ and B^{3+} drastically changed. The distance of travel of A^+ was very much extended into the soil, while the amount of B^{3+} replaced was small. Consequently, the concentration of B^{3+} in solution was low. However, the maximum distance of travel of B^{3+} was the same as that observed when $k = 1$ or $k = 10$. The left side of the curve was broadly extended, while its right side was kept unchanged.

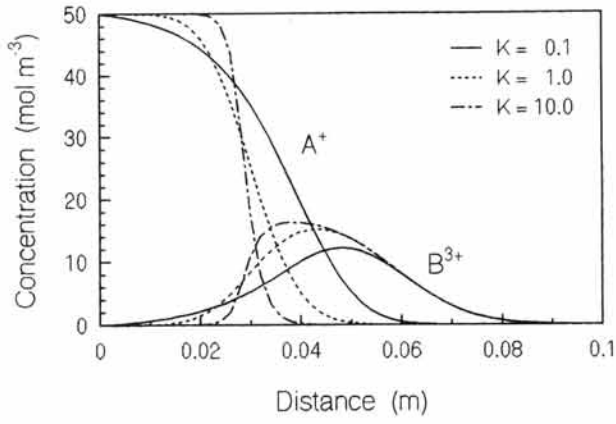

Fig. 2. Effect of exchange equilibrium constant on the distributions of A^+ and B^{3+} in solution at t = 6×10^4s.

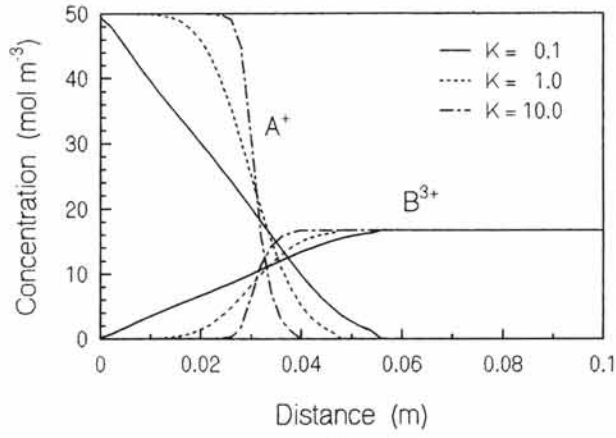

Fig. 3. Distributions of A^+ and B^{3+} in exchanger at t = 6×10^4s with same parameters except K = 0.1, 1, and 10.

When the value of K was increased to 10, the displacement boundary was sharper than that observed when $k = 1$. In addition, the maximum concentration of B^{3+} was a little greater and the position of the maximum was far behind compared to the results at $k = 1$. On the left side of the curve, a larger concentration gradient of B^{3+} (sharper curve) was developed, thus making distribution curve of B^{3+} skewed to the left. The distance over which B^{3+} traveled at the chosen time was also the same as that calculated using $k = 0.1$ or $k = 1$, while a retardation in the movement of A^+ was observed with the formation of sharper concentration gradient at the advancing front.

In general, since ion exchangers such as soil prefer counter ions of higher valence, the velocity at which A^+ traveled was faster as k decreased. The greater the equilibrium constant, the sharper the slope of the advancing front of A^+ and, as a result, more B^{3+} was displaced. This phenomenon was clearly seen in Fig. 3, in which the distributions of both A^+ and B^{3+} adsorbed at soil exchanger under the same condition given in Fig. 2 was represented.

The magnitude of the displacement of S_B by S_A in the

exchanger phase was governed by the value of k (Fig. 3). When the value of k was chosen to be unity, the pattern of distribution of the adsorbed ion, S_A, was similar to that of A^+ in Fig. 1. At every corresponding position behind the intersection of two distribution curves of A^+ and B^{3+} in the exchanger, the equivalent sum of both species was 50 mol m^{-3}, which satisfies the cation exchange capacity of the soil. Behind this position, the equivalent sum of A^+ and B^{3+} in the solution was also 50 mol m^{-3} (Fig. 2). The slope along the displacement boundary of the distribution curve of B^{3+} adsorbed on the exchanger, S_B, at the corresponding time was the same as that along the left side of the distribution of B^{3+} in the solution phase (Fig. 2). Under this condition (i.e., k = 1), as Eq. (4) indicates, the equivalent concentration ratio of A^+ to B^{3+} adsorbed on the exchanger, $\{(S_A)^3/(S_B)\}$, at any given time and position should be equal to that in the solution phase, $\{(A^+)^3/(B^{3+})\}$.

If the k was 10, the displacement of S_B was sharper than that obtained using k = 1, and the magnitude of advancement of S_A was greater than that of A^+ in the solution at the corresponding positions near the displacement front. This implies all B^{3+} was virtually displaced from the exchanger even before the concentration of advancing A^+ reached 50 mol m^{-3}. In this situation, the slope of displacement boundary of S_B was the same as that of the left side of the distribution of B^{3+} in the solution (Fig. 2). The quotient of the equivalent concentration ratios of A^+ to B^{3+} in the exchanger and in the solution should hold tenfold, thus allowing B^{3+} adsorbed on the exchanger to be easily displaceable.

A very distinct pattern of distribution of S_A and S_B was obtained when k was 0.1. The spatial distribution of S_A was high at the left inlet boundary and decreased linearly. Unlike the spatial distribution of S_A when $k = 1$ or $k = 10$, its maximum concentration plateau around the left boundary did not appear. This phenomenon was also observed in the distribution of A^+ in the solution phase using $k = 0.1$ (Fig. 2). On the other hand, the spatial distribution of B^{3+} adsorbed on the exchanger showed a virtually linear decrease towards the left boundary. This result indicates that the displacement of S_B by A^+ was not very effective when the value of K was much smaller than unity. As Eq. (7) implies, the amount of S_A, which replaced S_B, became zero, as the value of k approached zero. Thus, the spatial distribution patterns of A^+ and B^{3+} in the solution phase (Fig. 2) and in the exchanger phase (Fig. 3) showed the relative amounts of S_A and S_B were greatly governed by the value of k and the relative concentrations of A^+ and B^{3+}, as Eq. (4) indicates.

Influence of cation exchange capacity. When the magnitude of R was reduced to 25 mol m^{-3}, the average velocity of A^+ was 6.7×10^{-7} m s^{-1}, which is nearly two thirds that of pore water. Because the chosen value of R was small as compared to A_o, the penetration of the displacing ion extended to greater depths. Under this condition, the amount of B^{3+} displaced and the concentration of the maximum at the fixed time were reduced, compared to those shown in Fig. 1. On the other hand, the average velocity of B^{3+} on the

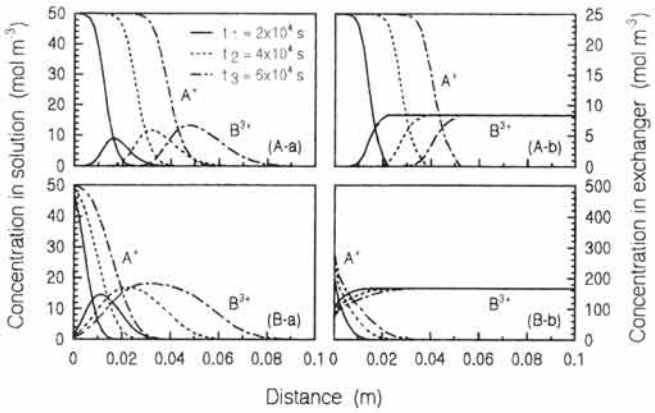

Fig. 4. Distributions of A^+ and B^{3+} in (a) solution and (b) exchanger at three different times with same parameters except for R = 25 mol m^{-3} (A) and 500 mol m^{-3} (B).

left side of the maximum was the same as that of advancing A^+ (6.7×10^{-7} m s^{-1}), while the right side of the maximum traveled at the same velocity of pore water (1×10^{-6} m s^{-1}). As indicated elsewhere, this discrepancy in the velocities of both sides caused the position of the maximum of B^{3+} to travel with the velocity of 8 x 10^{-7} m s^{-1} (Fig. 4A-a), which is slightly faster than that observed in Fig. 1. The distance of separation of the adjacent curves of A^+ and B^{3+} was also nearly equal on the left side of the maxima.

The spatial and temporal distribution of the two cation species adsorbed on the exchanger is shown in Fig. 4A-b. Under this condition, the displacement of S_B was very effective and the magnitude of advancement of S_A was slightly less than that of A^+ at the corresponding positions near the displacement front, since the concentration equivalent to R was chosen as one half that of inlet concentration (A_o). Consequently, virtually all B^{3+} was displaced from the soil exchanger behind this displacement boundary. This implies that the cation species in soil would be readily displaced from the surface provided that the concentration of the displacing ion exceeding that of cation exchange capacity was maintained for sufficient time. However, the reverse situation in which the displacing ion with relatively low concentration is intermittently fed into a soil of higher exchange capacity is common.

If the value of R was 500 mol m^{-3} (i.e., 10 cmol kg^{-1}), the average velocity of A^+ was greatly retarded to less than 2.5×10^{-7} m s^{-1}, which is nearly one quarter that of pore water and the distance between the adjacent curves of A^+ was shorter (Fig. 4B). Under this condition, the average velocity of B^{3+} on the left side was nearly the same as that of A^+, while that on the right side also moved with the same velocity of pore water. Therefore, the advancement of the B^{3+} displaced at a given time was the same as that of pore water with any R value, since the uniformly decreasing concentration gradient was established ahead of its maximum once displacement of S_B was initiated. The travel of A^+ was very much retarded, while the amount of B^{3+} replaced was large. Consequently, the concentration of B^{3+} in the solution was high. The

maximum concentration of B^{3+} was higher than that observed when R = 25 mol m^{-3} or R = 50 mol m^{-3}.

Another distinct feature appeared in the spatial and temporal distribution patterns of B^{3+} in the solution (Fig. 4B-a). With time, B^{3+} was much extended into the column with the left skirt of its distribution fixed firmly at the surface, while that obtained when R = 25 mol m^{-3} migrated along the column, indicating that A^+ did not displace S_B entirely from the uppermost part of the exchanger. This phenomenon was more evident with the distribution pattern of S_A and S_B on the exchanger (Fig. 4B-b); the displacement of S_B by A^+ was not completed in the uppermost part of the column. As seen in Fig. 4B-b, as long as the fraction of S_A on the exchanger is less than unity, the displacement of S_B by A^+ would be always incomplete.

Anion concentration profile and mass balance. During transport of cation species through soils, their positive charge should be electrically compensated by the equivalent negative charge carried by anion species in the soil. This electroneutrality condition should be satisfied everywhere in the column. Thus, at a given time, the total equivalent sum of A^+ and B^{3+} in the solution phase should correspond to that of a common anion species and this envelope calculated as the sum of two cation species should be also identical to that of displacing ion, A^+, when R = 0. In this case, A^+ advanced as far as that of pore water (1×10^{-6} m s^{-1}), thus indicating that it did not interact with B^{3+} on the exchanger and could travel at the same velocity. Moreover, as long as the parameters such as dispersion coefficient and pore water velocity were kept constant, the anion concentration profile with any choice of *k* or R was the same at a given time, thus it was excluded here. The invariant concentration profile of anion indicated that the model accounted for instantaneous charge balance fairly well.

If a solution, with A_0 = 50 mol m^{-3}, was constantly fed into the cross-sectional area of 1×10^{-4} m^2 at the velocity of 1×10^{-6} m s^{-1}, the total amount of A^+ applied to the soil column during t = 6×10^4s would be 0.300 mmol. The total equivalent of each cation species in solution and in the adsorbed phase was calculated from the results using the trapezoidal rule and that of anion was obtained by summing those of A^+ and B^{3+} in the solution phase.

At t = 6×10^4s, the equivalent of A^+ and B^{3+} in the solution and in the exchanger was calculated as 0.151 mmol and the total equivalent of cation species in the solution was equal to that of anion species in the solution and to that of A^+ and S_A. Thus, the ratio of the total equivalent of A^+ and S_A to that of displacing ion, A^+, applied during the termination time was 1.00 with less than 1% relative error, which is attributable to the cumulative computational error. In particular, the total equivalent of B^{3+} displaced into solution by A^+ was the same as that of B^{3+} in the solution. Corresponding equivalent fractions of S_A and S_B in the exchanger were 30.2 and 69.8%, respectively.

In general, the microscopic Peclet number has often been evaluated to determine if an equilibrium for either exchange or adsorption was attained during miscible-displacement experiments in aggregated soil.[15] Even though no experimental observation was made to verify the model, the microscopic Peclet number for the CEC of 25 mol m^{-3} was evaluated. The maximum pore water velocity at the advancing front of A^+ was 6.7×10^{-7} m s^{-1}, the maximum radius of soil aggregates was assumed to be 1.0 mm (the upper limit of soil particle), and the minimum diffusion coefficient of the ionic species involved was 1×10^{-9} m^2 s^{-1}. Using these values, the Peclet number was found to be 0.67. This number less than unity indicates that sufficient time for diffusion of displacing ion into the soil aggregates was available during transport.

Although mass balance error less than 1% from 5 simulation results (overall balance sheet is excluded here) indicates that this model operated effectively, this study lacks experimental evaluation of the model. In addition to binary ion exchange between monovalent and non-hydrolyzed trivalent cation species described in this study, further consideration should be given to the protonation due to hydrolysis of trivalent cation, the appropriate exchange selectivity coefficient equation, the resultant multi-component cation exchange, and the variable pH-dependent CEC. Nevertheless, this study shows an applicability of the model as a subroutine subprogram provided that overall cation exchange is definable as a combination of multiple binary ion exchanges.

Acknowledgments. We are sincerely grateful to Dr. C.M. Cho, Dep. of Soil Science, University of Manitoba, Canada for his helpful comments and suggestions after reviewing an earlier draft of this paper.

References

Lindsay, W. L. (1979) In *Chemical Equilibria in Soils*, pp. 39-41, John-Wiley & Sons, New York, NY.

Mansell, R. S., Bond, W. J. and Bloom, S. A. (1993) Simulating cation transport during water flow in soil: Two approaches. *Soil Sci. Soc. Am. J.* **57**, 3-9.

Rubin, J. and James, R. V. (1973) Dispersion-affected transport of reacting solutes in saturated porous media: Galerkin method applied to equilibrium controlled exchange in unidirectional steady water flow. *Water Resour. Res.* **9**, 1332-1356.

Helfferich, F. (1962) In *Ion Exchange*, pp. 156-158, McGraw Hill, New York, NY.

Snyder, V. A. and Cavallaro, N. (1997). The thermodynamic of ion exchange: a single-phase mixture formulation. *Soil Sci. Soc. Am. J.* **61**, 36-43.

Elprince, A. M., Vanselow, A. P. and Sposito, G. (1980) Heterovalent, ternary cation exchange equilibria: NH_4^+-Ba^{2+}-La^{3+} exchange on montmorillonite. *Soil Sci. Soc. Am. J.* **44**, 964-969.

Bond, W. J. and Philips, I. R. (1990) Ion transport during

unsteady water flow in an unsaturated clay soil. *Soil Sci. Soc. Am. J.* **54**, 636-645.

Bond, W. J. and Verburg, K. (1997) Comparison of methods for predicting ternary exchange from binary isotherms. *Soil Sci. Soc. Am. J.* **61**, 444-454.

Förster, R. (1986) A multicomponent transport model. *Geoderma* **38**, 261-278.

Reuss, J. O. and Johnson, D. W. (1986) In *Acid Deposition and the Acidification of Soils and Waters*, Springer-Verlag, New York, NY.

Cotton, F. A. and Wilkinson, G. (1988) In *Advanced Inorganic Chemistry* (5th ed.) pp. 962-963, John-Wiley & Sons, New York, NY.

Beyer, W. H. (1984) In *CRC Standard Mathematical Tables* (27th ed.) pp. 9, CRC Press Inc., FL.

Cho, C.M. (1985) Ionic transport in soil with ion-exchange reaction. *Soil Sci. Soc. Am. J.* **49**, 1379-1386.

Lapidus, L. and Pinder, G. F. (1982) In *Numerical Solution of Partial Differential Equations in Science and Engineering*, pp. 160-161 and 214-218, John-Wiley & Sons, New York, NY.

Bond, W. J. and Philips, I. R. (1990) Cation exchange isotherms obtained with batch and miscible displacement techniques. *Soil Sci. Soc. Am. J.* **54**, 722-728.